

Conducting rod on the axis of a charged ring: The Kelvin water drop generator

Gorazd Planinšič and Tomaž Prosen

Physics Department, University of Ljubljana, Jadranska 19, 1111 Ljubljana, Slovenia

(Received 24 May 1999; accepted 6 April 2000)

The problem of calculating the induced surface charge density along the finite length grounded conducting rod placed on the axis of the charged ring is solved numerically and compared with the experimental results. Two cases are considered in the theoretical treatment: the ring connected to a constant potential and the ring carrying a constant charge. The problem is related to the optimization of the Kelvin water drop electrostatic generator. A simple experiment is presented which gives reliable measurements of the induced charge density at the end of the conducting rod. © 2000 American Association of Physics Teachers.

I. PLAYING WITH THE KELVIN WATER DROPPER

Some time ago an article about the Kelvin water dropper¹ came to our attention and we decided to construct a water dropper in the first-year project lab. The device, schematically shown in Fig. 1, is in principle an electrostatic voltage generator that works as follows.

The water drops fall from both outlets above the conducting rings *A* and *B*. Suppose the conducting ring *A* initially has a slightly negative charge. Then a positive charge will be induced in the water at the outlet above ring *A* and the positively charged drops will fall into the can *P*. Since the can *P* is connected to the ring *B*, this will bring more positive charge on the ring *B*, making the drops falling into the can *R* be charged more negatively. The story goes on. In this way the potential difference between the isolated branches continually increases.

Though there are several articles about the Kelvin water dropper, we found only one touching on the improvement of the geometry of the apparatus.² One may ask, for instance, what is the optimal radius of the charged ring compared to the size of the can where water is collected, what is the optimal separation between the ring and the can, etc. We focused on the following question: What should be the position of the water outlet relative to the charged ring to produce maximal induced charge on the water drops? The problem was tackled experimentally (measuring the induced charge on the drops versus water outlet-charged ring separation) and theoretically. In this article we present the theoretical treatment and the experimental results.

II. THEORY

We have chosen the conducting ring and the grounded conducting rod on the axis of the ring for our model (Fig. 2). The choice of the grounded conducting rod is justified by the symmetry of the apparatus: the two outlets carry equal and opposite charges, therefore the midpoint (water reservoir) may be grounded. Two cases are treated: the ring carrying a constant charge and the ring connected to a constant potential.

A. The ring carrying a constant charge

First we calculate the induced surface charge density on the rod $\sigma_s(z)$ for an arbitrary ring-to-rod separation. The induced charge on the drops as a function of ring-to-rod

separation can then be found since the charge on the water drop leaving the lower end of the rod is proportional to the charge density at this end of the rod.

Let the ring and the rod be placed in the coordinate system as shown in Fig. 2. The electric field on the axis of a ring with the radius *a* carrying a charge q_0 can be expressed as

$$E_0(z) = \frac{\sigma_0 z a^2}{4 \epsilon_0 (a^2 + z^2)^{3/2}}, \quad (1)$$

where

$$\sigma_0 = \frac{q_0}{\pi a^2}.$$

The corresponding potential on the *z* axis is

$$U_0(z) = \frac{\sigma_0 a^2}{4 \epsilon_0 \sqrt{a^2 + z^2}}. \quad (2)$$

The derivation of expressions (1) and (2) is a good exercise for first-year students. Observing $E_0(z)$, one might expect that the induced charge on the water drops would be maximal if the lower end of the rod where the drops are dripping off were placed at the maximum of $E_0(z)$ (that is, $\sqrt{2}a$ from the ring center). As will be shown later, this is not the case.

Let us assume in the further calculation that

- (1) the radius of the ring *a* is much larger than the radius of the rod *p*: $a \gg p$,
- (2) the radius of the ring is much larger than the thickness of the ring wire ρ : $a \gg \rho$,
- (3) the length of the rod *L* is much larger than the radius of the rod: $L \gg p$.

From the third assumption, we can neglect the charge induced on the two circular base surfaces of the rod. The induced charge on the cylindrical surface of the rod creates on the *z* axis an electric potential that can be calculated by integrating the differential contributions of small charged rings along the length of the rod. Using the expression for the potential of the charged ring (2), the potential of the rod placed on the *z* axis as shown in Fig. 2 can be expressed in the following form:

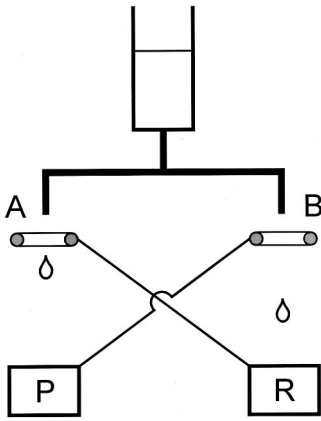


Fig. 1. The Kelvin water dropper.

$$U_s(z) = \int_{b-L}^b \frac{\sigma_s(z') p dz'}{2\epsilon_0 \sqrt{p^2 + (z-z')^2}}, \quad (3)$$

where b is the coordinate of the lower end of the rod and $\sigma_s(z')$ is the induced charge density in quest. Note that b is negative in Fig. 2.

The total potential U_{tot} created by the charged ring and by the induced charges on the grounded conducting rod in the arbitrary point on the z axis is the sum of expressions (2) and (3). By measuring all the lengths in units of the ring radius a , the total potential can be written in the following form:

$$U_{\text{tot}}(u) = \frac{\sigma_0 a}{4\epsilon_0 \sqrt{1+u^2}} + \frac{a}{2\epsilon_0} \int_{\beta-\lambda}^{\beta} \frac{\sigma_s(u') \eta du'}{\sqrt{\eta^2 + (u-u')^2}}, \quad (4)$$

where

$$u = \frac{z}{a}$$

and

$$\beta = \frac{b}{a}, \quad \lambda = \frac{L}{a}, \quad \eta = \frac{p}{a}. \quad (5)$$

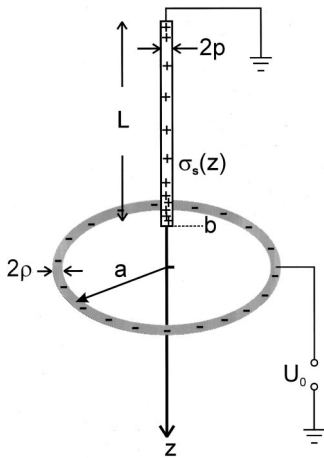


Fig. 2. The scheme of the experiment. The presence of the charge q_0 on the ring induces a surface charge density $\sigma_s(z)$ on the grounded conducting rod. Two cases are treated: the ring carrying a constant charge and the ring connected to a constant potential U_0 .

When the rod is grounded, $U_{\text{tot}}(u)=0$ along the whole rod and Eq. (4) can finally be expressed as

$$\int_{\beta-\lambda}^{\beta} \frac{\sigma_s(u') \eta du'}{\sqrt{\eta^2 + (u-u')^2}} = -\frac{\sigma_0}{2\sqrt{1+u^2}}, \quad (6)$$

where $\beta-\lambda \leq u \leq \beta$. Solving this equation means finding the appropriate function $\sigma_s(u)$ which satisfies the equality.

Though Eq. (6) cannot be solved analytically, it can be approximated in this situation, as shown in Ref. 3. One can approximate

$$\int \frac{\sigma_s(u') du'}{\sqrt{\eta^2 + (u-u')^2}} \approx \sigma_s(u) \int \frac{du'}{\sqrt{\eta^2 + (u-u')^2}} \quad (7)$$

because, when $\eta \ll 1$, the integrand is negligible except near $u'=u$. The latter integral can be done exactly in terms of logarithms

$$\int_{\beta-\lambda}^{\beta} \frac{du'}{\sqrt{\eta^2 + (u-u')^2}} = \ln \left(\frac{u-\beta + \sqrt{\eta^2 + (u-\beta)^2}}{u-\beta + \lambda + \sqrt{\eta^2 + (u-\beta + \lambda)^2}} \right) \quad (8)$$

and therefore the surface charge density on the rod can be expressed as

$$\sigma_s(x) = \frac{\sigma_0}{2\eta} \left[\sqrt{1 + (\beta - \lambda + \lambda x)^2} \times \ln \left(\frac{x-1 + \sqrt{(\eta/\lambda)^2 + (x-1)^2}}{x + \sqrt{(\eta/\lambda)^2 + x^2}} \right) \right]^{-1}, \quad (9)$$

where the x coordinate is defined as

$$x = \frac{z - (b-L)}{L} = \frac{u - (\beta - \lambda)}{\lambda} \quad (10)$$

and lies in the interval $0 \leq x \leq 1$. Note that this approximation will not be good near the ends because $\sigma_s \rightarrow \infty$ there. Since the surface charge density at the end of the rod is exactly what we are searching for, we cannot use the approximate solution and we must solve Eq. (6) numerically. The integral on the left-hand side of Eq. (6) can be replaced by the sum of the finite number of terms evaluated in the discrete points. Let us choose N equidistant points on the axis along the rod. Then the u coordinate becomes the discrete variable

$$u_i = \beta - \lambda \frac{N-i}{N-1}, \quad (11)$$

which runs along the whole rod when index i runs from 1 to N . The distance between two points of the mesh is

$$du = \frac{\lambda}{N-1}.$$

If we replace u and u' with u_i and u_j , Eq. (6) takes the form

$$\sum_{j=1}^N \frac{\sigma_s(u_j) \eta}{(N-1) \sqrt{\left(\frac{\eta}{\lambda}\right)^2 + \left(\frac{i-j}{N-1}\right)^2}} = -\frac{\sigma_0}{2\sqrt{1+u_i^2}}. \quad (12)$$

Note that we used the definition (11) and that λ has been brought into the denominator of the left-hand side of the equation. This equation represents a system of N linear equations with N variables. The variables are unknown values of

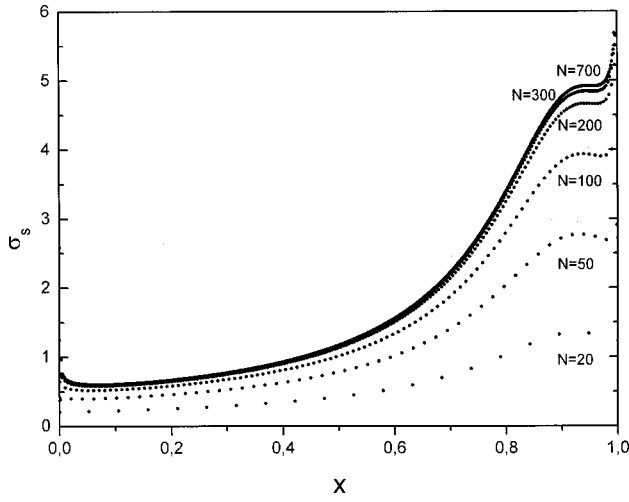


Fig. 3. The dependence of calculated surface charge density on the number of mesh points used in the numerical calculation, where x is defined in Eq. (10). In this example, $\beta=0.5$, $\lambda=6.4$, $\eta=0.01$ and condition (19) requires $N>640$.

the induced charge density σ_s at the discrete points u_j . We may use the compact notation

$$\sigma_j = \sigma_s(u_j), \quad (13)$$

$$p_i = -\frac{\sigma_0}{2\sqrt{1+u_i^2}}, \quad (14)$$

$$r_{ij} = \frac{\eta}{(N-1)\sqrt{\left(\frac{\eta}{\lambda}\right)^2 + \left(\frac{i-j}{N-1}\right)^2}}, \quad (15)$$

and rewrite Eq. (12) as

$$\sum_{i=1}^N \sigma_j r_{ij} = p_i, \quad (16)$$

or in matrix form

$$\mathbf{R}\boldsymbol{\sigma} = \mathbf{p}. \quad (17)$$

The unknown vector $\boldsymbol{\sigma}$ can be calculated as

$$\boldsymbol{\sigma} = \mathbf{R}^{-1}\mathbf{p}. \quad (18)$$

How many points do we have to choose on the rod to obtain a reliable result? Since we calculated the potential of the rod as the integral of small charged ring contributions, the minimum number of points N should be large enough so that the separation between two adjacent points is smaller than the rod radius, or

$$N > \frac{\lambda}{\eta}. \quad (19)$$

For our experimental parameters ($\lambda=6.4$, $\eta=0.01$), condition (19) requires $N>640$. Therefore the number of points (and the number of equations) readily exceeds a few hundred. Luckily, several software packages are available that can solve similar problems. Our results were obtained with MATHEMATICA 4.0. The example shown in Fig. 3 illustrates how the result in this case depends on the number of mesh points used in the numerical calculation.

B. The ring connected to a constant potential

In this case the charge on the ring is a function of the ring-to-rod separation. The charge density on the rod is still given by the solution of the previous problem apart from the unknown scaling factor proportional to the charge on the ring. The charge on the ring $q_0(\beta)$ is constrained by the additional condition that the ring potential is U_0 . This condition can be expressed as

$$\int_{a+\rho}^{\infty} E_r dr = U_0, \quad (20)$$

where E_r is the radial component of the total electric field, a is the mean radius of the ring, and ρ is the ring wire radius. Since $E_r = E_r^{\text{ring}} + E_r^{\text{rod}}$, the integration can be split into two terms. The term E_r^{ring} (the radial component of the electric field created by the ring at the distance r in the plane of the ring) can be expressed as the integral of the point charge contributions around the ring

$$E_r^{\text{ring}}(r') = \frac{q_0(\beta)}{4\pi^2\epsilon_0 a^2} \int_0^\pi \frac{(r' - \cos\varphi)d\varphi}{((r' - \cos\varphi)^2 + \sin^2\varphi)^{3/2}}, \quad (21)$$

where $r' = r/a$. In a similar way, E_r^{rod} can be expressed in the following form:

$$E_r^{\text{rod}}(r') = \frac{\eta}{4\epsilon_0} \int_{\beta-\lambda}^\beta \frac{\sigma_s(u)r' du}{(r'^2 + u^2)^{3/2}}, \quad (22)$$

where $u = z/a$ and the rest of the variables have the same meaning as in the previous paragraph. Combining expressions (20)–(22) gives the equation

$$\frac{q_0(\beta)}{4\pi^2\epsilon_0 a^2} \int_{1+\nu}^{\infty} dr' \int_0^\pi \frac{(r' - \cos\varphi)d\varphi}{((r' - \cos\varphi)^2 + \sin^2\varphi)^{3/2}} + \frac{\eta}{4\epsilon_0} \int_{1+\nu}^{\infty} dr' \int_{\beta-\lambda}^\beta \frac{\sigma_s(u)r' du}{(r'^2 + u^2)^{3/2}} = U_0, \quad (23)$$

where $\nu = \rho/a$. The integrals with respect to r' can be analytically solved in both terms, reducing Eq. (23) to

$$\frac{q_0(\beta)}{4\pi^2\epsilon_0 a} \int_0^\pi \frac{d\varphi}{\sqrt{\sin^2\varphi + (1+\nu - \cos\varphi)^2}} + \frac{a\eta}{4\epsilon_0} \int_{\beta-\lambda}^\beta \frac{\sigma_s(u)du}{\sqrt{(1+\nu)^2 + u^2}} = U_0. \quad (24)$$

In our experiment the ring wire radius is much smaller than the ring radius. For this reason ν in the second term of Eq. (24) can be neglected compared to unity. The integral in the first term will be designated by $H(\nu)$ and can be expressed in the following form.

$$H(\nu) = \int_0^\pi \frac{d\varphi}{\sqrt{[(1+\nu)^2 + 1] - 2(1+\nu)\cos\varphi}} = \frac{2}{\nu} K\left[-\frac{4}{\nu^2}(1+\nu)\right], \quad (25)$$

where K is the complete elliptic integral of the first kind. Since $\nu \ll 1$, in our case $H(\nu)$ in Eq. (25) is well approximated by $\ln(8/\nu)$ (see Ref. 4). Some results of the numerical

Table I. $H(\nu)$.

ν	$H(\nu)$	$\ln \frac{8}{\nu}$
0.1	4.2217	4.382
0.01	6.6564	6.685
0.001	8.9832	8.987
0.0001	11.2893	11.290

calculation of $H(\nu)$ and corresponding approximate values are given in Table I.

Equation (24) can now be expressed in the final form

$$\frac{q_0(\beta)}{4\pi^2\epsilon_0 a} H(\nu) + \frac{a\eta}{4\epsilon_0} \int_{\beta-\lambda}^{\beta} \frac{\sigma_s(u) du}{\sqrt{(1+u^2)}} = U_0. \quad (26)$$

As described above, the solution of the problem $\sigma_s(u)$ can be scaled:

$$\sigma_s(u) = \tilde{\sigma}_s(u) \sigma_0(\beta), \quad (27)$$

where $\tilde{\sigma}_s(u)$ is the solution of the problem with fixed unity charge density on the ring described in the previous section, Eq. (6):

$$\int_{\beta-\lambda}^{\beta} \frac{\tilde{\sigma}_s(u') \eta du'}{\sqrt{\eta^2 + (u-u')^2}} = -\frac{1}{2\sqrt{1+u^2}}. \quad (28)$$

Using Eq. (26) and the notation $\sigma_0(\beta) = q_0(\beta)/\pi a^2$, the charge density $\sigma_0(\beta)$ can be expressed as

$$\sigma_0(\beta) = \frac{4\epsilon_0 U_0}{a} \left[\frac{H(\nu)}{\pi} + \eta \int_{\beta-\lambda}^{\beta} \frac{\tilde{\sigma}_s(u) du}{\sqrt{1+u^2}} \right]^{-1}. \quad (29)$$

Combining Eqs. (27) and (29) gives the final solution in the form

$$\sigma_s(u) = \tilde{\sigma}_s(u) \frac{4\epsilon_0 U_0}{a} \left[\frac{H(\nu)}{\pi} + \eta \int_{\beta-\lambda}^{\beta} \frac{\tilde{\sigma}_s(u) du}{\sqrt{1+u^2}} \right]^{-1}. \quad (30)$$

Again the integral in Eq. (30) can be replaced by the summation and the equation written in the following discrete form:

$$\sigma_s(u_j) = \tilde{\sigma}_s(u_j) \frac{2\epsilon_0 U_0}{a} \left[\frac{H(\nu)}{2\pi} + \eta \lambda \sum_{i=1}^N \frac{\tilde{\sigma}_s(u_i)}{(N-1) \sqrt{1 + \left(\beta - \lambda \frac{i-1}{N-1} \right)^2}} \right]^{-1}. \quad (31)$$

The calculation of the charge density $\sigma_s(u_j)$ on the rod using Eq. (31) goes as follows: For given parameters β and ν , the function $H(\nu)$ and the unity charge density $\tilde{\sigma}_s(u_j)$ are calculated first. The latter is the result of the problem solved in the previous paragraph. Once these are known, the charge density on the rod can be calculated using Eq. (31).

If we focus on Eq. (29), we notice that the presence of the rod is described only by the second term in brackets. There-

Table II. Numerical values of B [see Eqs. (29) and (33)] for the several ring-to-rod separations in our experimental setup ($\eta=0.01$, $\lambda=6.4$, $\nu=0.01$). The corresponding value of the term A is 2.128.

β	B
-1	2.585×10^{-2}
-0.5	3.983
-0	5.922
0.5	7.586
1	8.462
1.5	8.758
2	8.50
2.5	7.734

fore, by dropping this term from Eq. (29), the self-capacitance of the ring alone can be expressed in the form

$$C_{\text{ring}}^0 = \frac{4\pi^2\epsilon_0 a}{H(\nu)}. \quad (32)$$

Let us compare the two terms in the brackets of Eq. (29) for our experiment. The configuration of our experiment has the following parameters, $\eta=0.01$, $\lambda=6.4$, $\nu=0.01$, and the ring was connected to a constant potential (see Fig. 4). The two terms are denoted by

$$A = \frac{H(\nu)}{\pi}, \quad B = \eta \int_{\beta-\lambda}^{\beta} \frac{\tilde{\sigma}_s(u) du}{\sqrt{1+u^2}}, \quad (33)$$

and their numerical values for several ring-to-rod separations are summarized in Table II. In our case the error made by neglecting the B term in calculating $\sigma_s(u_j)$ from Eq. (31) is less than 4%. Therefore, in our experiment the charge on the ring does not change much with the ring-to-rod separation and can be regarded as constant.

III. EXPERIMENT

The important part of the experiment is the detector that measures the charge on the water drops. We used the ingenious rain drop charge measuring device presented some time ago in Scientific American.⁵ For our purpose we had to reduce the gain of the amplifier by a factor of 24 and we had to put an additional grounded cylindrical shield around the sensor in order to suppress a 50-Hz hum. The instrument works on the principle of electrical induction. A charged drop falling through a metal cylinder will momentarily induce a charge on the cylinder. The electronic circuit measures this charge and gives an output voltage spike whose peak value is proportional to the charge on the drop:

$$q_{\text{drop}} = K \frac{U_{\text{peak}}}{\sqrt{1 + (D/L)^2}}, \quad (34)$$

where D and L are the diameter and the length of the inner cylinder of the sensor and K is the sensor constant. In our case, $D/L=0.73$ and $K=2.4 \times 10^{-11}$ As/V. The experimental setup is schematically shown in Fig. 4.

We used a long brass tube with 2 mm outside diameter as a conducting rod and a 200-mm-diam copper ring as a charge carrying ring. The upper end of the brass tube was connected to the inverted soda bottle with a plastic tube. The water flow of approximately 2 drops per second was adjusted with a small plastic pipe (all standard hospital material). The brass tube was fixed to the vertical positioner. Measurements

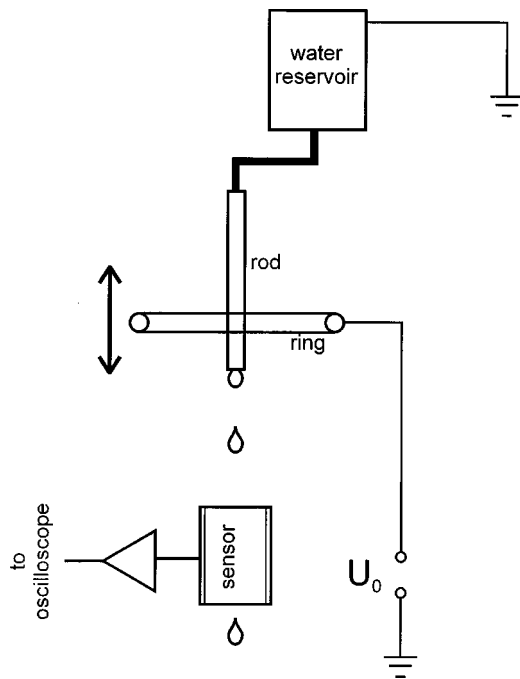


Fig. 4. The experimental setup for measuring the induced charge on the water drops falling off the thin brass tube that is placed on the axis of the charged ring.

were done by moving the brass tube along the axis of the copper ring and recording the charge measured on the water drops at each position. The ring was connected to a high voltage source and the water in the soda bottle was grounded.

We also tried to experiment with the charged ring, but the charge leakage from the ring prevented a reliable measurement. However, as shown in the previous section, the capacitance between the ring and the brass tube is practically independent of the ring-to-tube separation. This means that in our experiment the net charge on the ring can also be considered as constant in the case when the ring is connected to a constant-voltage source.

IV. RESULTS

The calculated induced surface charge density on the grounded rod at the various ring-to-rod separations is shown in Fig. 5. In the calculation, the ring charge density σ_0 was set to minus unity. Note that the parameter β measures the coordinate of the lower end of the rod and that the ring center coincides with the center of a coordinate system. For instance, $\beta=1$ means that the lower end of the rod is one ring radius below the ring center (see Fig. 2). The results show that if the ring center lies within the rod length, this causes accumulation of the induced charge on the rod close to the ring center (marks $\beta=0.5$ and $\beta=1$ in Fig. 5). This effect is combined with a steep rise of the induced charge at the ends of the rod.

The dependence of the charge on the falling drops on ring-to-rod separation is shown in Fig. 6, where both the theoretical curve and the measured values are presented on the same graph. The measured values for each point in the graph were reproducible and stable within 5%.

Since detailed geometry of the drop has not been considered in our theoretical treatment, the theoretical values of the

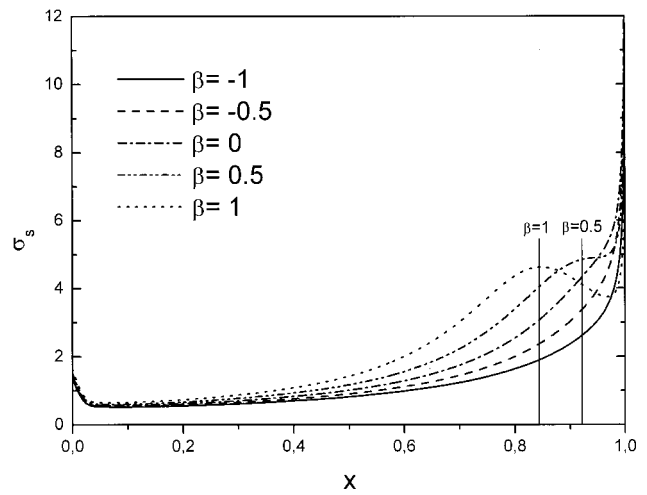


Fig. 5. The results of the numerical calculation of the induced surface charge density along the rod at various ring-to-rod separations. Two vertical lines mark the position of the ring center relative to the rod (only $\beta>0$ cases are marked). The ring charge density σ_0 was set equal to unity and other parameters were $\lambda=6.4$, $\eta=0.01$, and $N=700$.

charge on the falling drop can be compared with experimental values within the scaling factor. On the graph in Fig. 6, the scaling factor was determined to give the best fit with the measured points. The results show that the optimal ring-to-rod separation β_{opt} (at which the induced charge on the falling drops is largest) is achieved when the lower end of the rod is placed slightly above the ring center.

However, the estimation of the charge on the falling drop can be done using Eq. (30) and numerically calculated values $\bar{\sigma}_s(u_i)$. Neglecting the integral in Eq. (30) and taking $H(\nu)$ from Table I, the charge on the drop falling from the end of the rod can be estimated as

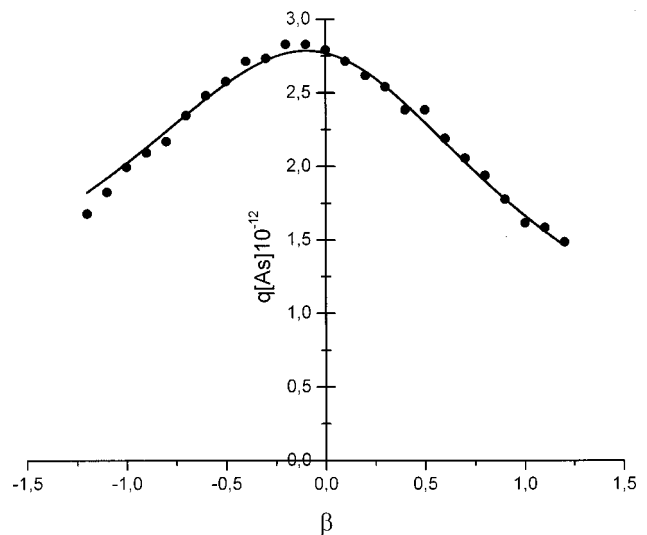


Fig. 6. The comparison between the calculated (smooth line) and the measured (circles) induced charge on the falling drops as function of the ring-to-rod separation. The parameters used in the experiment and in the simulation were $\eta=0.01$ and $\lambda=6.4$. The ring radius was 0.1 m and it was connected to a 120-V potential. The theoretical values were multiplied by a scaling factor so that the best fit with the experimental values has been obtained. Calculation of the induced surface charge density on the rod has been done with 700 points.

$$q_{\text{drop}} = \frac{8\pi^2\epsilon_0 a U_0 \eta \lambda}{H(\nu)N} \sum_{i=1}^M \bar{\sigma}_s(u_i), \quad (35)$$

where M is the size of the drop in terms of the step of discretization. For our experimental parameters $\beta=0$, $\lambda=6.4$, $\nu=0.01$, $U_0=120$ V, $a=0.1$ m, and $N=700$, the estimated charge on a 4-mm-diam drop is 5.6×10^{-12} As. As can be seen from the graph, the corresponding measured value 2.8×10^{-12} As is of the same order of magnitude.

We have not done further measurements but the computed results suggest that β_{opt} moves higher above the ring center and the corresponding charge density at the end of the rod decreases when the ratio η grows (i.e., increasing the outlet tube diameter). However, the practical value of this result is limited by the initial assumption that $\eta \ll 1$ and by the fact that the shape of the drop has not been considered in our theoretical treatment.

V. CONCLUSIONS

With the aim to optimize the Kelvin water dropper, the problem of calculating the induced surface charge density along the grounded conducting rod placed on the axis of a charged ring has been treated. The results show that the induced charge on the rod accumulates close to the center of

the ring (if the center lies on the rod) and at the ends of the rod. The performance of the Kelvin electrostatic generator is therefore maximized if the water outlet is placed in the center of the charging ring, provided that the diameter of the tube is much smaller than the diameter of the ring. The measured and the calculated values of the induced charge on the falling drops are in reasonable agreement, despite the fact that the shape of the water drop has not been considered in our treatment. The use of the Kelvin electrostatic generator in combination with the water drop charge measuring device proved to be a helpful hands-on experiment in teaching and learning electrostatics. Demonstrations such as the exponential growth of the generated charge and the conservation of charge can also be shown using the same apparatus and will be described elsewhere.

¹Paul Chagnon, "Animated Displays. VI. Electrostatic Motors and Water Dropper," *Phys. Teach.* **34**, 491–494 (1996).

²Se-yuen Mak, "The Kelvin Water-Drop Electrostatic Generator—An Improved Design," *Phys. Teach.* **35**, 549–551 (1997).

³Mark Andrews, "Equilibrium charge density on a conducting needle," *Am. J. Phys.* **65**, 846–850 (1997).

⁴M. Abramowitz and A. Stegun, *Handbook of Mathematical Functions* (Dover, New York, 1972).

⁵"Getting a Charge out of Rain," *The Amateur Scientist*, *Sci. Am.* **277** (8), 64–65 (1997).